

PREDICTION OF FATIGUE CRACK GROWTH RATE IN CORRODED REINFORCEMENT BARS

MUNEEM AHMAD DAR*, PERVAIZ FATHIMA K. M. †

Indian Institute of Technology Jammu (IIT Jammu)
NH-44, PO Nagrota, Jagti, Jammu and Kashmir 181221
www.iitjammu.ac.in

*e-mail: muneem.dar@iitjammu.ac.in

†e-mail: pervaiz.khatoon@iitjammu.ac.in

Key words: Corrosion Fatigue, Reinforced Concrete, Fatigue crack Propagation, Paris law Constants.

Abstract. Reinforced concrete structures are widely used in construction due to their strength and durability. However, in corrosive environments, corrosion-induced degradation can reduce the cross-sectional area and strength of the reinforcement, ultimately resulting in structural failure. Corrosion pits in the reinforcement bar can act as stress amplifiers, causing localised stress concentration, thereby initiating the growth of fatigue cracks when subjected to cyclic loading. The Paris law is widely used to model fatigue crack propagation in metallic materials. It relates the crack growth rate under cyclic loading to the stress intensity factor range through the material constants C and m . The fatigue crack growth rate is typically divided into three stages, where the Paris law is valid in the second stage. In this work, stage-I and stage-II are modelled using a linear and power law (Paris law) relationship respectively. Existing studies have shown that the commonly accepted value of the Paris law constants significantly underestimates the fatigue life of reinforced concrete structures in corrosive environments. In this study, the crack growth coefficients for both stage-I and stage-II are ascertained in an inert environment and a corrosive medium under varying stress ratios. An empirical relationship between the constants for inert and corrosive environments is obtained. Thus knowing the crack growth constants of the material in air, fatigue crack growth rate in corrosive environments can be predicted.

1 INTRODUCTION

Chloride contamination is the primary cause of corrosion in reinforced concrete (RC) structures, significantly reducing their durability [1]. Persistent erosion from the environment and repeated vehicle loads result in corrosion fatigue damage in RC bridges for highways and railways [2, 3]. The combination of corrosion and fatigue drastically reduces the expected lifespan of these important structures [5–7]. Understanding the interaction between corrosion and fatigue is essential for maintaining and repairing these structures [8–10]. Fatigue cracks tend

to initiate at relatively low cyclic stress levels, often at pre-existing surface defects, the roots of rebar ribs, and corrosion-induced pits [4]. The progression of these cracks, known as corrosion fatigue crack propagation (CFCP), significantly influences the interplay between material degradation caused by corrosion and fatigue [11]. The fact that fatigue cracks can readily initiate at weak points such as corrosion-induced pits is noteworthy. The sudden failure of tension reinforcement, which is the leading cause of fatigue failure under corrosion fatigue, is one manifestation of this detrimental com-

bination [12]. In fact, the majority of the fatigue life of a material is focused on the initiation and growth of fatigue cracks [13]. In addition, the corrosion surrounding steel bars affects the fatigue crack growth rate [14]. The manner in which reinforced and pre-stressed concrete columns fail due to fatigue is also related to how the reinforcing bars fail [15]. The development of small and large cracks within reinforcing bars has a significant contribution to the effects of fatigue on concrete structures [16]. The growth of fatigue cracks is influenced by a number of factors, including how frequently the stress changes and the surrounding environment of the crack. These changes can be both external (such as the size of the crack) and internal (such as the composition of the material) [17]. Since the 1960s, researchers have investigated the relationship between the lowest and highest stress (stress ratio) and the rate at which cracks develop. Corrosion of the steel bars in concrete bridges is one of the most common causes of their failure [1]. To build robust concrete structures, it is essential to understand how steel reinforcement deteriorates due to fatigue, particularly from corrosion. The ongoing effort to understand the effects of corrosion on steel bars is essential because it can significantly impact the durability of concrete bridges over time [15].

The fatigue crack propagation (FCP) can be divided into three stages: near-threshold FCP (I stage), stable FCP (II stage), and unstable FCP (III stage) as illustrated in Fig. 1(a). Because the unstable period frequently lasts for few fatigue loading cycles, it is commonly neglected in fatigue studies. As a result, research has focused on the first two stages [17]. When the failure occurs prematurely at a lower stress level and a smaller number of load cycles, under the combined action of fatigue loading and corrosion, than that would be expected in the absence of the corrosive environment is referred to as coupled corrosion fatigue phenomenon [18]. The threshold stress intensity factor for CFCP, denoted as K_{thcf} , is observed to be smaller compared to the threshold stress intensity, denoted as K_{th} , governing FCP in a chemically in-

ert environment, particularly evident in cases of true corrosion fatigue as illustrated in Fig. 1(b). This is because the corrosive medium reduces the material's resistance to FCP. The CFCP rate is remarkably higher than it would be in an inert environment once the applied stress intensity range reaches K_{thcf} . The CFCP rate gradually approaches the FCP rate in an inert environment as ΔK rises.

In this study, the fatigue crack growth rate curve of the reinforcing bar under a corrosive environment is predicted based on the fatigue crack growth rate curve of the reinforcing bar in an inert environment. The stage-I and stage-II of the fatigue crack growth rate curve of the rebar in air and corrosive medium are modelled using linear and power law relations respectively. A correlation between constants in the air and those from the corrosive medium is developed using the empirical fitting, after observing trends in the coefficients across different stress ratios. This enables predicting fatigue crack growth in corrosive environment based on inert medium crack propagation data, establishing a connection between fatigue crack growth and corrosion. The proposed model offers a means to quantify fatigue crack evolution in reinforced concrete structures that are affected by corrosion in aggressive environments.

2 ANALYSIS OF CORROSION FATIGUE CRACK GROWTH RATE

The literature [19] presents experimental CFCP plots of hot-rolled ribbed bar, with a nominal yield strength of 400 MPa (HRB400), characterised as a form of low-carbon steel. This particular steel variant corresponds to the Grade 60 ribbed rebar classification in ASTM A615 (ASTM 2009). HRB400 finds extensive application in concrete bridges, making it a fitting choice for our research context and hence was used for the analysis of crack propagation in the current study.

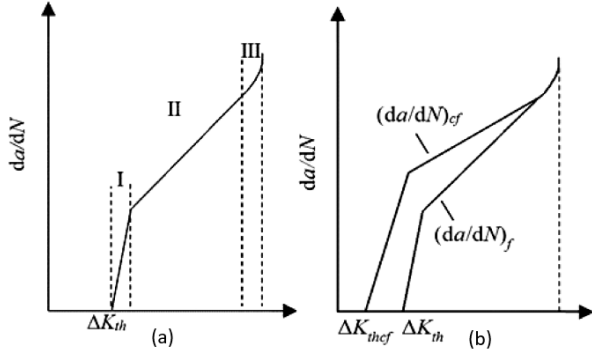


Figure 1: Corrosion fatigue Crack growth (a) three stages of the FCP (b) True CFCP [19]

The test employed specially processed single-edge notched bending SEN(B) specimen obtained from the reinforcing bar through milling and wire cutting with the design of the test specimen adhering to the specifications outlined in ASTM E647 (ASTM 2013) and is shown in Fig. 2.

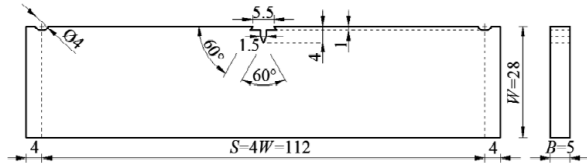


Figure 2: Single-edge notched bending specimen geometries (millimetres) [19]

The FCP tests were conducted following ASTM E647 (ASTM 2013) specifications, with two key factors: the environment (air, 3.5 % NaCl solution) and load ratio (0.1, 0.2, 0.3, 0.5, and 0.7). Tests were done on a fatigue machine using a sinusoidal load at 10 Hz [19].

The FCP (da/dN versus ΔK) curve was divided into two distinct parts; the initial part is called the near-threshold FCP (Stage I) and the second part is termed stable FCP (Stage II). The minimum slope criterion successfully demarcates the two parts, as the slope changes abruptly between the two regions and can be easily visualised in Fig. 1b.

The plots for stress ratios 0.1, 0.2 and 0.3 were selected for fitting constants separately for the two regions of the curve in an inert (air) and

corrosive medium (3.5% NaCl solution) [19]. The curve fitting for the first two stages is described below.

Stage-I

$$\left(\frac{da}{dN}\right)_{\text{air}}^{(I)} = m_1^{\text{air}} \Delta K + C_1^{\text{air}} \quad (1)$$

$$\left(\frac{da}{dN}\right)_{\text{NaCl}}^{(I)} = m_1^{\text{NaCl}} \Delta K + C_1^{\text{NaCl}} \quad (2)$$

Stage-II

$$\left(\frac{da}{dN}\right)_{\text{air}}^{(II)} = C_2^{\text{air}} \Delta K^{m_2^{\text{air}}} \quad (3)$$

$$\left(\frac{da}{dN}\right)_{\text{NaCl}}^{(II)} = C_2^{\text{NaCl}} \Delta K^{m_2^{\text{NaCl}}} \quad (4)$$

The constants for both the stages and environments are given in Table 1 and Table 2 for the different stress ratios.

3 MODELLING OF FATIGUE CRACK GROWTH RATE

Upon comparing the constants of the FCP of corrosive and inert environments, under different stress ratios, both in Stage I and Stage II as tabulated in Table 1 and Table 2, respectively, a trend is observed. This relationship between the constants in inert and corrosive environments as a function of the stress ratio are plotted in Figs. 3-6.

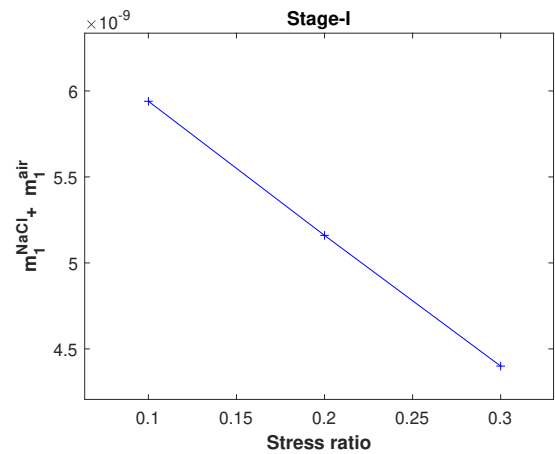


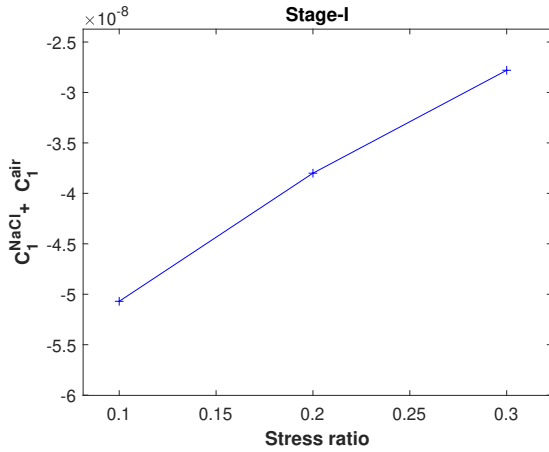
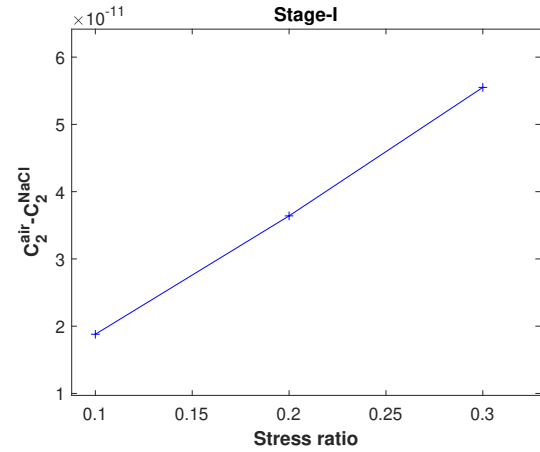
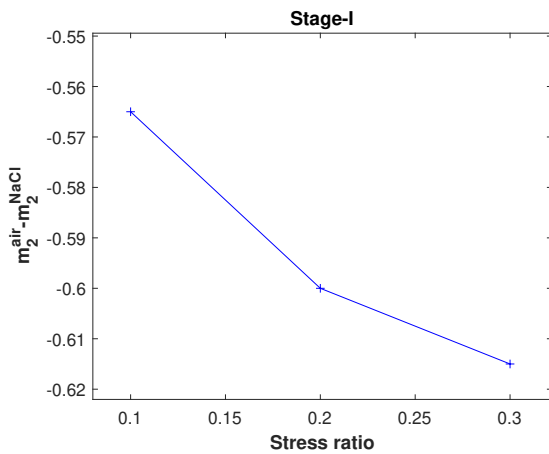
Figure 3: Trend observed in the constant m of Stage-I

Table 1: Constants for Stage I of the Curve in Air and NaCl solution.

m_1^{air}	m_1^{NaCl}	$m_1^{air} + m_1^{NaCl}$	C_1^{air}	C_1^{NaCl}	$C_1^{air} + C_1^{NaCl}$
2.71E-09	3.23E-09	5.94E-09	-2.56E-08	-2.51E-08	-5.07E-08
2.54E-09	2.62E-09	5.16E-09	-2.07E-08	-1.73E-08	-3.80E-08
2.00E-09	2.40E-09	4.40E-09	-1.44E-08	-1.34E-08	-2.78E-08

Table 2: Constants for the Stage II of the Curve in Air and NaCl solution.

m_2^{air}	m_2^{NaCl}	$m_2^{NaCl} - m_2^{air}$	C_2^{air}	C_2^{NaCl}	$C_2^{NaCl} - C_2^{air}$
3.1	2.535	-0.565	3.40E-12	2.22E-11	1.88E-11
3	2.4	-0.6	3.56E-12	4.00E-11	3.64E-11
2.965	2.35	-0.615	4.47E-12	6.00E-11	5.55E-11


Figure 4: Trend observed in the constant C of Stage-I

Figure 6: Trend observed in the constant C of Stage-II

Figure 5: Trend observed in the constant m of Stage-II

The observation from Figs.3-6 shows the influence of environmental conditions on crack propagation behaviour. Subsequently, a correlation was fitted between the constants in air and the corrosive medium for the two distinct segments of the crack growth curve. These correlations reveal how materials and their surroundings interact, helping us understand the processes governing crack growth. The resulting relationships are given by Eqs. 5-8

For stage-I, we have

$$m_1^{NaCl} = 9.059 \times 10^{-9} R^2 - 1.096 \times 10^{-8} R + 6.947 \times 10^{-9} m_1^{air} \quad (5)$$

Eq. 2 and 4 therefore we get

$$C_1^{\text{NaCl}} = -1.33 \times 10^{-7} R^2 + 1.562 \times 10^{-7} R - 6.45 \times 10^{-8} - C_1^{\text{air}} \quad (6)$$

Similarly, for the stage-II, we have

$$m_2^{\text{NaCl}} = 0.2876 R^2 - 0.3885 R - 0.623 + m_2^{\text{air}} \quad (7)$$

$$C_2^{\text{NaCl}} = -1.244 \times 10^{-10} R^2 + 2.1632 \times 10^{-10} R - 1.096 \times 10^{-12} + C_2^{\text{air}} \quad (8)$$

$$\left(\frac{da}{dN} \right)_{\text{NaCl}}^{(I)} = (9.059 \times 10^{-9} R^2 - 1.096 \times 10^{-8} R + 6.947 \times 10^{-9} - m_1^{\text{air}}) \Delta K \quad (9)$$

$$+ (-1.33 \times 10^{-7} R^2 + 1.562 \times 10^{-7} R - 6.45 \times 10^{-8} - C_1^{\text{air}})$$

$$\left(\frac{da}{dN} \right)_{\text{NaCl}}^{(II)} = (-1.244 \times 10^{-10} R^2 + 2.1632 \times 10^{-10} R - 1.096 \times 10^{-12} + C_2^{\text{air}}) \quad (10)$$

$$\Delta K^{(0.2876 R^2 - 0.3885 R - 0.623 + m_2^{\text{air}})}$$

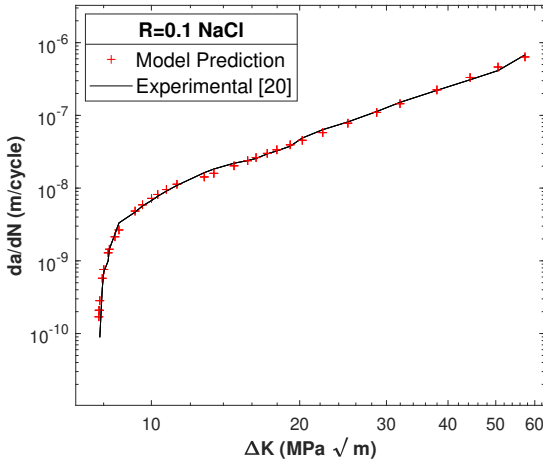


Figure 7: Crack growth rate (da/dN versus ΔK) relationships in NaCl at a load ratio of 0.1

The crack growth rate in NaCl is given by Eq. 2 and Eq. 4 for Stage-I and Stage-II respectively. Substituting the values of m_1, m_2, C_1 and C_2 from Eqs. 5-8 respectively in

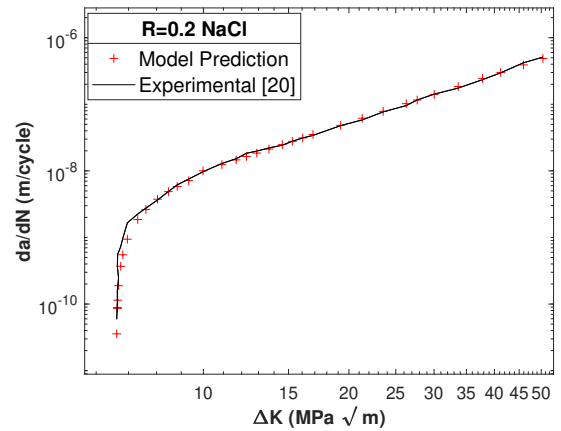


Figure 8: Crack growth rate (da/dN versus ΔK) relationships in NaCl at a load ratio of 0.2

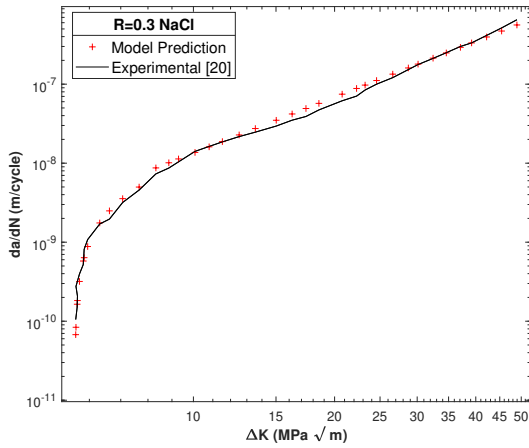


Figure 9: Crack growth rate (da/dN versus ΔK) relationships in NaCl at a load ratio of 0.3

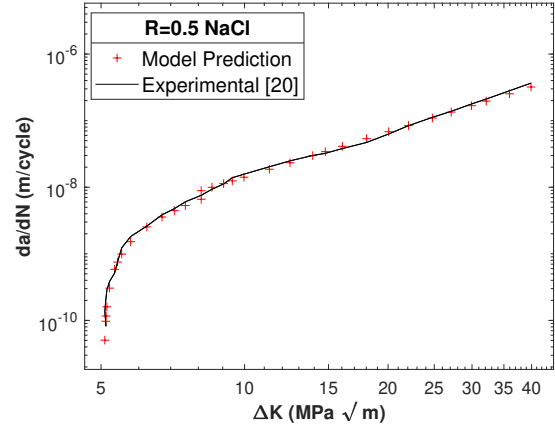


Figure 10: Crack growth rate (da/dN versus ΔK) relationships in NaCl at a load ratio of 0.5

The crack growth rate curves were calibrated for the stress ratios 0.1, 0.2 and 0.3, and are shown in Figs. 5-9. These are the same stress ratios for which the constants were fitted as well.

4 VALIDATION OF THE PROPOSED MODEL

The proposed model is used to predict crack growth rate in corrosive environment for stress ratios 0.5 and 0.7 and compared with the respective experimental fatigue crack growth rate curves [19] to validate the model. Figs.10-11 show the predicted curves depicting CFCP rates along with experimental observations. The comparison distinctly highlights a strong agreement between the CFCP rates projected by the proposed model and the observed experimental results.

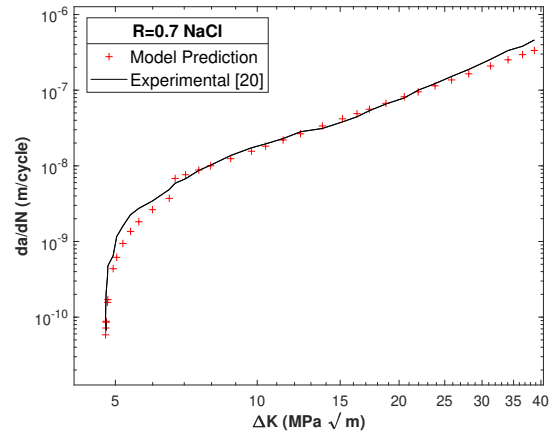


Figure 11: Crack growth rate (da/dN versus ΔK) relationships in NaCl at a load ratio of 0.7

5 CONCLUSIONS

An empirical model to predict the CFCP rate of reinforcing bars is proposed. The model considers the effect of stress ratio and corrosive environment on the behaviour of the fatigue crack growth rate curve. The variation of crack growth constants with stress ratio in the corrosive environment and inert environment are related. Results showed that the constants displayed differing trends in Stage I and Stage II of the FCP curve. The model may be further refined considering additional experimental observations.

REFERENCES

- [1] Ma, Y., Guo, Z., Wang, L., Zhang, J. (2017) investigation of corrosion effect on bond behavior between reinforcing bar and concrete., *Construction and Building Materials*, 152, 240-249.
- [2] Ma, Y., Guo, Z., Wang, L., Zhang, J. (2020). Probabilistic life prediction for reinforced concrete structures subjected to seasonal corrosion-fatigue damage., *Journal of Structural Engineering*, 146(7), 04020117.
- [3] Apostolopoulos, C. A., Demis, S., Papadakis, V. G. (2013). Chloride-induced corrosion of steel reinforcement–Mechanical performance and pit depth analysis., *Construction and Building Materials*, 38, 139-146.
- [4] Angst, U. M., Geiker, M. R., Michel, A., Gehlen, C., Wong, H., Isgor, O. B., ... Buenfeld, N. (2017) The steel–concrete interface., *Materials and Structures*, 50, 1-24.
- [5] Stewart, M. G., Al-Harthy, A. (2008). Pitting corrosion and structural reliability of corroding RC structures: Experimental data and probabilistic analysis., *Reliability engineering system safety*, 93(3), 373-382.
- [6] Apostolopoulos, C. A. (2010). Coastal bridges and the 120 Life Span–the Rio-Antirio case study., *International Journal of Structural Integrity*, 1(2), 173-183.
- [7] Ma, Y., Xiang, Y., Wang, L., Zhang, J., Liu, Y. (2014). Fatigue life prediction for aging RC beams considering corrosive environments., *Engineering Structures*, 79, 211-221.
- [8] Guo, Z., Ma, Y., Wang, L., Zhang, J. (2019). Modelling guidelines for corrosion-fatigue life prediction of concrete bridges: Considering corrosion pit as a notch or crack., *Engineering Failure Analysis*, 105, 883-895.
- [9] Yi, W. J., Kunnath, S. K., Sun, X. D., Shi, C. J., Tang, F. J. (2010). Fatigue Behavior of Reinforced Concrete Beams with Corroded Steel Reinforcement., *ACI Structural Journal*, 107(5).
- [10] Ma, Y., Guo, Z., Wang, L., Zhang, J. (2020). Probabilistic life prediction for reinforced concrete structures subjected to seasonal corrosion-fatigue damage., *Journal of Structural Engineering*, 146(7), 04020117.
- [11] Song, Q. N., Zheng, Y. G., Ni, D. R., Ma, Z. Y. (2015). Characterization of the corrosion product films formed on the as-cast and friction-stir processed Ni-Al bronze in a 3.5 % wt NaCl solution., *Corrosion*, 71(5), 606-614.
- [12] Bastidas-Arteaga, E., Bressolette, P., Chateauneuf, A., Sánchez-Silva, M. (2009). Probabilistic lifetime assessment of RC structures under coupled corrosion–fatigue deterioration processes., *Structural safety*, 31(1), 84-96.
- [13] Yang, D. H., Yi, T. H., Li, H. N. (2017). Coupled fatigue-corrosion failure analysis and performance assessment of RC bridge deck slabs., *Journal of Bridge Engineering*, 22(10), 04017077.
- [14] Ma, Y., Wang, G., Su, X., Wang, L., Zhang, J. (2018). Experimental and modelling of the flexural performance degradation of corroded RC beams under fatigue load. *Construction and Building Materials*, 191, 994-1003.
- [15] Guo, Z., Ma, Y., Wang, L., Zhang, X., Zhang, J., Hutchinson, C., Harik, I. E. (2020). Crack propagation-based fatigue life prediction of corroded RC beams considering bond degradation. *Journal of Bridge Engineering*, *Journal of Bridge Engineering*, 25(8), 04020048.

- [16] Ray, S., Kishen, J. C. (2014). Analysis of fatigue crack growth in reinforced concrete beams. *Materials and structures* Materials and structures, 47, 183-198.
- [17] Ramsamooj, D. V., Shugar, T. A. (2001). Modeling of corrosion fatigue in metals in an aggressive environment. *International Journal of Fatigue*, 23, 301-309.
- [18] Kovalov, D., Fekete, B., Engelhardt, G. R., Macdonald, D. D. (2019). Prediction of corrosion fatigue crack growth rate in alloys. Part II: Effect of electrochemical potential, NaCl concentration, and temperature on crack propagation in AA2024-T351. *Corrosion Science*, 152, 130-139.
- [19] Ma, Y., Liu, X., Guo, Z., Wang, L., Lu, N. (2021). Predicting corrosion fatigue crack propagation behavior of HRB400 steel bars in simulated corrosive environments. *Journal of Materials in Civil Engineering*, 33(6), 04021127.